Surface-peaked medium sensitivity of the optical potential: an exact result

H.F. Arellano†‡*, F.J. Aguayo*† *and E. Bauge*‡
†Physics Department - FCFM, University of Chile, Blanco Encalada 2008, Santiago, Chile
‡CEA DAM DIF, 91297 Arpajon CEDEX, Bruyères-le-Châtel, France

Abstract
Microscopic optical model potentials for elastic hadron-nucleus scattering usually take the form of a convolution of a two-body effective interaction with the target ground-state mixed density. Within the Brueckner-Bethe-Goldstone g-matrix approach for the effective interaction, nuclear medium effects are made explicit by means spatial integrals throughout the bulk of the nucleus. In this contribution we discuss a novel and exact approach to track down the manifestation of intrinsic nuclear medium effects. After examining the momentum- and coordinate-space structure of a two-body effective interaction –spherically symmetric in its *mean* coordinate– it is demonstrated that the intrinsic medium effects in the optical potential depend solely on the *gradient* of a reduced interaction. This feature implies the confinement of intrinsic medium effects to regions where the density varies most, i.e. the nuclear surface. This finding may be of special significance in the study of nuclear collisions sensitive to the peripheric structure of nuclei. We illustrate some of its implications in the context of $^{10}Be + p$ elastic scattering at 39.1A MeV.

1 Introduction

Common approaches for the construction of a microscopic optical model potential (OMP) for nucleon-nucleus (*NA*) scattering result in the folding of an antisymmetrized nucleon-nucleon (*NN*) effective interaction with the target ground-state mixed density of the nucleus. Even though models based on the Brueckner-Bethe-Goldstone (BBG) g matrix account for a broad body of scattering data [1, 2], there remain puzzling limitations –specially at nucleon energies below 100 MeV– which require further attention. This is specially relevant considering current trends aiming to the study of radioactive isotope beams colliding against hydrogen targets. When the energies of these unstable beams reach 100A MeV, the physics behind the collision mechanisms is the same as that of *NA* scattering at 100 MeV, typical nucleon energies explored in the seventies. Thus, current activities involving radioactive beams provide a stimulating ground to revisit the challenges to describe the interaction of nucleons with nuclei.

To quote some of these shortcomings we mention the calculated differential cross sections for NA scattering at energies below 60 MeV, which lack an adequate consistency when considering different targets or energies below 80 MeV [1, 3]. Another case is the Ramsauer effect exhibited by the total cross sections for neutron-nucleus scattering. Although some success has been reported in the description of this phenomena at energies as low as 65 MeV [4], the microscopic description of the cross section at lower energies and heavy targets remains an open problem [5]. In quasi-elastic *(p,n)* charge-exchange reactions to the isobaric analog state, the use of the full-folding optical potentials cannot account properly for the forward-angle (Fermi) cross sections, underestimating it by factors as large as of five [6]. From a theoretical point of view, these shortcomings call for a closer scrutiny of the way microscopic OMP are being calculated, addressing issues such as the adequacy of the effective interaction and/or the accuracy of simplifying assumptions needed in their current realizations. Some progress along these lines has been reported recently, where a closer scrutiny of the OMP in momentum space yields some novel features in the structure of the OMP.

2 The *unabridged* optical potential

The collisions between a nucleon with energy E and a composite target can be described by means of an OMP, a one-body operator which in momentum space takes the general form [7]

$$U(\boldsymbol{k}', \boldsymbol{k}; E) = \int d\boldsymbol{p}'\, d\boldsymbol{p}\, \langle \boldsymbol{k}'\boldsymbol{p}' \mid \hat{T}(E) \mid \boldsymbol{k}\, \boldsymbol{p} \rangle\, \hat{\rho}(\boldsymbol{p}', \boldsymbol{p})\;, \qquad (1)$$

with $\hat{T}$ a two-body effective interaction which, in general, contains information about the discrete spectrum of the many-body system. The one-body mixed density in momentum space, $\hat{\rho}(\boldsymbol{p}', \boldsymbol{p})$, represents the ground-state structure of the target. A complete evaluation of the optical potential considering all these elements is far from feasible with current computing capabilities. Part of the difficulties can be avoided if one treats separately the target ground-state and the *NN* effective interaction, a reasonable strategy for intermediate and high energy collisions. A remaining difficulty is to account for the Fermi motion of the target nucleons, present in the $d\boldsymbol{p}\, d\boldsymbol{p}'$ integration.

As demonstrated in Ref. [8], the disentanglement of intrinsic medium contributions from its free-space counterpart stems from a general analysis of the momentum-space structure of the two-body effective interaction. The matrix elements of $\hat{T}$ in coordinate space are denoted with $\langle \boldsymbol{r}'\boldsymbol{s}' \mid \hat{T} \mid \boldsymbol{r}\;\boldsymbol{s}\rangle$, where the 'prior' coordinates of each particle are denoted by $\boldsymbol{r}$ and $\boldsymbol{s}$, respectively. Analogously, $\boldsymbol{r}'$ and $\boldsymbol{s}'$ refer to the 'post' coordinates of the same particles, as illustrated in Fig. (1). These vectors define the *mean coordinate* $\boldsymbol{Z}$, given by the simple average of the prior and post coordinates:

$$\boldsymbol{Z} = \tfrac{1}{4}(\boldsymbol{r} + s + r' + s')$$

In momentum space, the $\hat{T}$-matrix elements are denoted with $\tilde{T} \equiv \langle \boldsymbol{k}'\boldsymbol{p}' \mid \hat{T} \mid \boldsymbol{k}\;\boldsymbol{p}\rangle$, where $\boldsymbol{k}$ and $\boldsymbol{p}$ represent the projectile and struck-nucleon momenta prior to interaction, respectively. Analogous definitions, using prime marks, follow for the the post momenta. These two representations of the $\hat{T}$-matrix are related by means of Fourier transforms, which following Ref. [8] yields

$$\langle \boldsymbol{k}'\boldsymbol{p}' \mid \hat{T} \mid \boldsymbol{k}\;\boldsymbol{p}\rangle = \int \frac{d\boldsymbol{Z}}{(2\pi)^3}\, e^{i\boldsymbol{Z}\cdot\boldsymbol{K}_\perp} g_{\boldsymbol{Z}}(\boldsymbol{K}_\parallel; \boldsymbol{b}', \boldsymbol{b})\;. \qquad (2)$$

Here the *reduced interaction*, $g_{\boldsymbol{Z}}$, is evaluated at the mean coordinate $\boldsymbol{Z}$ and depends on the relative momenta $\boldsymbol{b}$ and $\boldsymbol{b}'$, and the current of the interacting pair momentum $\boldsymbol{K}_\parallel$. These vectors are given by

$$\begin{aligned}
\boldsymbol{b}' &= \tfrac{1}{2}[\boldsymbol{K} - \boldsymbol{P} - \tfrac{1}{2}(\boldsymbol{q} + \boldsymbol{Q})]\,; \\
\boldsymbol{b} &= \tfrac{1}{2}[\boldsymbol{K} - \boldsymbol{P} + \tfrac{1}{2}(\boldsymbol{q} + \boldsymbol{Q})]\,; \\
\boldsymbol{K}_\parallel &= \boldsymbol{K} + \boldsymbol{P}\,; \\
\boldsymbol{K}_\perp &= \boldsymbol{Q} - \boldsymbol{q}\;.
\end{aligned}$$

where we have denoted $\boldsymbol{q} = \boldsymbol{k}' - \boldsymbol{k}$, the projectile momentum transfer; $\boldsymbol{Q} = \boldsymbol{p} - \boldsymbol{p}'$, the momentum transferred to the target nucleon; $\boldsymbol{K} = (\boldsymbol{k} + \boldsymbol{k}')/2$, the projectile mean momentum; and $\boldsymbol{P} = (\boldsymbol{p} + \boldsymbol{p}')/2$, the target-nucleon mean momentum.

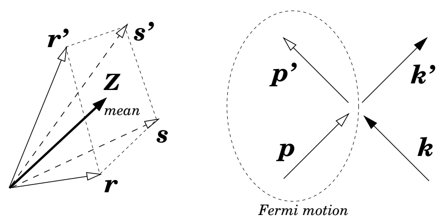

Fig. 1: Representation of the prior/post coordinates and momenta in a two-body operator.

At this point it is worthwhile to examine the particular case of a spherically symmetric finite nucleus. In such a case we assume that g_Z depends only on the magnitude of the mean coordinate, $|\boldsymbol{Z}| = Z$. Additionally, we assume that far away from the center of the nucleus the effective interaction g_Z tends to its free-space form $g_\infty \equiv t$. To simplicity the writing we omit the momentum arguments in the interaction g_Z and replace $g_Z = (g_Z - g_\infty) + g_\infty$, in Eq. (2). After performing the solid angle integration ($d\hat{Z}$) and subsequent integration by parts [8], we obtain the *asymptotic separation*

$$\tilde{T} = \delta(\boldsymbol{K}_\perp) g_\infty - \frac{1}{2\pi^2} \int_0^\infty Z^3 \, dZ \; \Phi_1(Z\, K_\perp) \, \frac{\partial g_Z}{\partial Z} \; , \tag{3}$$

where $\Phi_1(t) = j_1(t)/t$, with j_1 the spherical Bessel function of order 1. What is interesting about this result is that it disentangles very clearly the free-space contribution, the g_∞ term, from its medium-dependent counterpart. The medium dependence appears as the gradient of the reduced interaction, whereas the medium-independent contribution exhibits momentum conservation, as dictated by $\delta(\boldsymbol{K}_\perp)$: $\boldsymbol{K}_\perp = 0 \Rightarrow \boldsymbol{k} + \boldsymbol{p} = \boldsymbol{k}' + \boldsymbol{p}'$. The presence of a Z dependence in the reduced interaction inhibits momentum conservation in the $\hat{T}$ matrix. Momentum conservation is restored when $\partial g_Z / \partial Z = 0$, as in the cases of translationally invariant systems such as infinite nuclear matter or free space.

After replacing the above expression for $\tilde{T}$ into Eq. (1) for U we obtain the *unabridged* optical model potential, $U \equiv U_0 + U_1$, where

$$U_0(\boldsymbol{k}', \boldsymbol{k}; E) \;\; = \;\; \int d\boldsymbol{P} \hat{\rho}(\boldsymbol{q}; \boldsymbol{P}) t(\boldsymbol{K}_\parallel; \boldsymbol{b}', \boldsymbol{b}) \, ; \tag{4}$$

$$U_1(\boldsymbol{k}', \boldsymbol{k}; E) \;\; = \;\; \frac{1}{2\pi^2} \int d\boldsymbol{Q} \; d\boldsymbol{P} \hat{\rho}(\boldsymbol{Q}; \boldsymbol{P}) \int_0^\infty Z^3 dZ \Phi_1(Z|\boldsymbol{Q} - \boldsymbol{q}|) \left(- \frac{\partial g_Z}{\partial Z} \right) , \tag{5}$$

and $\hat{\rho}(\boldsymbol{Q}; \boldsymbol{P}) \equiv \hat{\rho}(\boldsymbol{p}', \boldsymbol{p})$. The term 'unabridged' has been coined here to indicate that the expression has not been subject to any simplifying consideration other than the spherical symmetry in the mean coordinate. All implicit non-localities and genuine momentum dependence off-shell are fully retained. Each matrix element of U involves a seven-dimensional integral, six of which account for the Fermi motion of the target nucleons ($d\boldsymbol{P} d\boldsymbol{Q}$), and one dimension for the radial integral on Z. Note that if $\partial g_Z / \partial Z = 0$, then $U \to U_0$, the free t-matrix limit of the *full-folding* optical potential introduced in the nineties to study *NA* scattering at intermediate energies [2].

Thus far we have made no allusion to any specific approach to model the $\hat{T}$ matrix, rendering the framework enough flexibility to investigate alternative approaches to represent the *NN* effective interaction in the realm of a finite nucleus. A realization of the optical can be made if we model the reduced interaction g_Z by means of the reaction matrix in the BBG theory for infinite nuclear matter. Here at each coordinate Z, where the local (diagonal) density of the nucleus is $\rho(Z)$, we identify the reduced interaction g_Z with the (antisymmetrized) reaction matrix. As demonstrated in Ref. [8], this model reproduces the *in-medium* folding model introduced by Arellano, Brieva and Love [3] if one assumes a Slater approximation for the mixed density. However, the above expression is general enough to allow the use of the full (off-shell) mixed density.

3 Surface-peaked medium effects

The medium-dependent term U_1 can be conveniently expressed as

$$U_1 = \int_0^\infty u(Z) \, dZ \; ,$$

with u representing a potential density. Thus, by examining the behavior of $u(Z)$ for selected matrix elements of U we can assess the importance of the various contributions to the OMP. For illustration purposes consider protons of mass m and energy E colliding against a given nucleus. We examine the

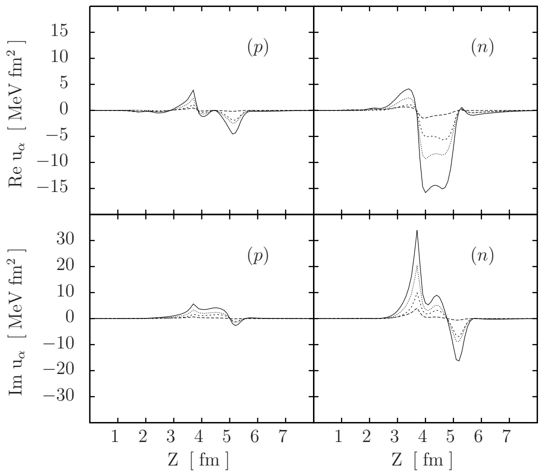

Fig. 2: Radial behavior of the potential density $u_\alpha(Z)$ for ^{16}O nucleus colliding with 30-MeV protons.

forward on-shell ($\boldsymbol{k} = \boldsymbol{k}'$; $k = \sqrt{2mE}$) matrix elements. Considering the case of ^{16}O, in Fig. (2) we plot the real (upper frames) and imaginary (lower frames) components of $u_\alpha(Z)$ for $E = 30$ MeV. Here the α label (dashed curves) represents, in decreasing order of importance, the $1p_{3/2}$, $1p_{1/2}$ and $1s_{1/2}$ shell contributions, while the solid curves represent the sum of all of them. The (*p*) and (*n*) labels symbolize couplings of the projectile (a proton) to the target protons and neutrons, respectively. Notice that the scale of Im u_α doubles that of Re u_α. This figure evidences quite neatly that medium effects become confined to the region $3 - 5.5$ fm, with clear dominance of the coupling to neutrons over those to protons. Judging from these figures, the inclusion/exclusion of proton densities in the evaluation of U_1 should have minor impact in the evaluation of the optical potential. In other words, the main sensitivity to intrinsic medium effects should come mainly from neutron densities.

To test these findings, we have evaluated optical potentials in the so-called $\delta g-$folding, namely, an approximation where the $\boldsymbol{Q}$ dependence of g_Z has been dropped by replacing $\boldsymbol{Q} \to \boldsymbol{q}$ in Eq. (5) [9]. This consideration allows a dramatic simplifications in the numerical evaluation of the optical potential, making it accessible with the use of personal computers. In Fig. (3) we show the calculated differential cross section for ^{10}Be + p elastic scattering at 39.1A MeV. The data are from Ref. [10]. Here the solid curves represent results within the $\delta g-$approach considering the two terms: $U_0 + U_1$. The dash-dotted curves correspond to the case where only U_0 is considered, namely the free t-matrix full-folding potential. The dashed (dotted) curves represent results where, in the evaluation of U_1, proton (neutron) matter distributions has been omitted. This selective switching illustrates clearly that the omission of neutron densities in the evaluation of U_1 has a major effect in the cross section, consistent with Fig. (2) for $u(Z)$. In contrast, the omission of proton densities renders minor effects in the cross sections, demonstrating its rather weak role in testing intrinsic medium effects. Overall, the description of the data provided by the $\delta g-$folding approach is reasonable but not yet satisfactory. It remains a pending issue to identify the source of the disagreements, particularly regarding the deeper minimum predicted by the theory but absent in the data. Work has been reported along these lines [10].

4 Summary and outlook

We have shown that the optical model potential can be expressed as the sum of two distinctive contributions: one depending on the free-space effective interaction and another depending on the gradient of a medium dependent effective interaction. When this medium dependence is modeled by means of the

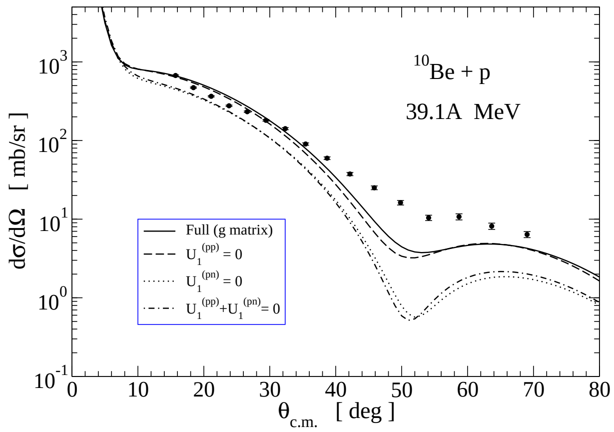

Fig. 3: Differential cross section for ^{10}Be$+n$ elastic scattering at 39.1A MeV. The data are from Ref. [10].

BBG reaction matrix we observe that the intrinsic medium effects of the interaction become confined to the nuclear surface, being this more pronounced in the case of the coupling of protons with neutrons. These findings, based on the assumption of spherical symmetry on the mean coordinate, have been assessed in the context of the δg-folding. These surface-sensitive phenomena, enhanced in the case of the peripheric neutrons, may be of particular importance in the study of rare isotope beams where exotic nuclei collide against hydrogen targets.

Acknowledgements

H.F.A. acknowledges partial funding provided by FONDECYT under grant 1080471.

References

[1] K. Amos, P. J. Dortmans, H. V. von Geramb, S. Karataglidis, and J. Raynal, Adv. in Nucl. Phys. **25**, 275 (2000).

[2] L. Ray, G. W. Hoffmann and W. R. Coker, Phys. Rep. **212**, 223 (1992).

[3] H. F. Arellano, F. A. Brieva, and W. G. Love, Phys. Rev. C **52**, 301 (1995).

[4] P. K. Deb, K. Amos, S. Karataglidis, M. B. Chadwick, and D. G. Madland, Phys. Rev. Lett. 86, 3248 (2001).

[5] H. F. Arellano and M. Girod, Phys. Rev. C **76**, 034602 (2007).

[6] H. F. Arellano and W. G. Love, Phys. Rev. C **76**, 014616 (2007).

[7] K. M. Watson, Phys. Rev. 89, 575 (1953).

[8] H. F. Arellano and E. Bauge, Phys. Rev. C **76**, 014613 (2007).

[9] F. J. Aguayo and H. F. Arellano, Phys. Rev. C **78**, 014608 (2008).

[10] N. Keeley and V. Lapoux, Phys. Rev. C 77, 014605 (2008).